Point-to-Point Comparison of Satellite and Ground-Based Cloud Properties at the ARM Southern Great Plains Central Facility

I. Genkova and C. N. Long
Pacific Northwest National Laboratory
Richland, Washington

P. Minnis
National Aeronautics and Space Administration
Langley Research Center
Hampton, Virginia

P. W. Heck
Cooperative Institute for Meteorological Satellite Studies
University of Wisconsin-Madison
Madison, Wisconsin

M. M. Khaiyer
Analytical Services and Materials, Inc.
Hampton, Virginia

Introduction

A complete four-dimensional (4D) characterization of a large-scale cloud field would be invaluable for better understanding and improved modeling of cloud processes at scales greater than a few kilometers. Surface-based instruments, such as a combination of radiometers and cloud lidars and radars, can provide detailed information on clouds above a particular location at high temporal resolution. Scanning lidars can be used to produce sequential images of three-dimensional (3D) cloud fields in limited situations over areas up to~70 km^2 providing small-area 4D cloud fields (e.g., Piironen and Eloranta 1995). The products that can be derived are limited and the imaging is confined to clouds with relatively small optical depths (ODs). Satellite data can provide total column properties over a large area and, while various inferences can be made about the vertical structure (e.g., Ho et al. 2003); the capability for deriving a reliable 3D cloud field from passive satellite measurements is limited. By using geostationary satellite data, such properties can be retrieved at a relatively high temporal resolution, providing the fourth dimension over a large scale.

Ou et al (2003) demonstrated that a detailed 3D cloud field can be estimated by using cloud radar to define the vertical structure of cloud properties within a column and then to link the vertical structure to total column retrievals of cloud properties from a satellite imager in order to apply the vertical structure to adjacent satellite pixels. The nominal result of that process is a 3D cloud field characterization over

an area that greatly exceeds the radar FOV, but remains small relative to the mesoscale domain. While such methods are promising, they are extremely limited because cloud radars, which are few in number, are needed for their implementation. Other, more widely available instruments that provide cloud information from the surface could be used together with satellite data to estimate the 3D cloud field over relatively large domains if the relationships between the surface and satellite data are quantified and the datasets are properly matched. Satellite and ground- or air-based measurements "meet" during the testing phase of these new techniques, since every new retrieval algorithm needs to be validated using the accepted or more sophisticated techniques that are available for interpreting or measuring clouds from a ground or aircraft platform.

Satellite data are comprised of discrete pixel radiances measured at a single instant in time while surface measurements can be taken at very high temporal resolutions, nearly continuously, but over a small area that could constant or variable depending on the FOV and the cloud structure. Because of these spatial and temporal differences in sampling between the satellite and surface measurements, temporal and spatial averages of the data are typically used to compare the same quantity derived from the respective points of view. Averaging over domains of different sizes is used to best meet the needs of a particular study resulting in a variety of approaches. For example, an atmospheric quantity observed from the surface would be averaged over a time interval corresponding to a certain distance dictated by the rate of advection of the quantity over the surface (e.g., Dong at al. 2002). Khaiyer at al. (2003) compared liquid water path (LWP) from a microwave radiometer (MWR) and the geostationary operational environmental satellite (GOES) visible infrared solar-infrared split-window technique (VISST) using the average for a swath of GOES pixels approximately corresponding to the portions of the cloud deck viewed by the MWR. In a study of ice water path (IWP) retrievals, Huang at al. (2003) compared half-hourly averaged surface-retrieved cloud properties with GOES radiances and retrieved cloud properties that were averaged in 0.3° boxes centered at each site. Min and Minnis (2004) compared both pixel and spatially averaged cloud properties derived from GOES to those from a sun-tracking radiometer situated at the Atmospheric Radiation Measurements (ARM; Ackerman and Stokes 2003) Program South Great Plains (SGP) Central Facility (SCF; 36.6°N, 97.5°W). In that study, it was necessary to select satellite pixels that were in the line of sight between the SCF and the sun. All these works agree that the time averaging is inevitable. However, many weather phenomena studies and climate analyses need finer scale information and, thus, data averaging does not improve the understanding of the physical processes when the original data are at roughly the same scale as the process.

One of the primary ARM objectives is to obtain measurements applicable to the development of models for better understanding of radiative processes in the atmosphere. To help meet that objective for mesoscale models, an effort is currently underway to build a 4D characterization of the cloud structure and properties over the greater SGP domain. Constructing a 4D characterization of clouds in a mesoscale domain using merged surface and satellite data requires refined matching of the surface and satellite observations to minimize the number of pixels that must be averaged. This need raises the question of how exactly to compare and interpret the data when it is put in conjunction with ground-based instrument derived data. This paper develops a technique for effective point-to-point comparison of satellite and ground-based cloud property retrievals. The technique is applied for comparing cloud amount and cloud OD and is used to determine the consistency between the two datasets.

Data and Methods

Ground-Based Retrievals

The ARM's SGP site is located over north-central Oklahoma and south-central Kansas. It operates one central, four boundary and twenty one extended facilities equipped with in situ and remote-sensing instruments. The SCF and each of the extended facilities run a Solar Infrared Radiation System (SIRS). The SIRS provides continuous measurements of downwelling and upwelling broadband shortwave (SW) and longwave (LW) irradiances. These 1-minute data are collected from the network of stations to help determine the total energy exchange within the SGP site (Stokes and Schwartz 1994).

Long at al. (1999) developed a SW Flux Analysis (SWFA) technique that utilizes the measured SW fluxes to determine how much optically thin and opaque cloud cover is present and determine the total amount of cloud cover, which is defined as SWFA hemispherical sky cover (SWFA SC). The SWFA SC was compared with the hemispherical cloud amounts from SCF total sky imager (TSI) to evaluate the SWFA method. The estimated SWFA SC uncertainty is ± 5% relative to the TSI cloud amount.

A simple empirical equation suggested by Barnard et al. (2003) is used to obtain a set of cloud ODs at the SCF for the same time period. It calculates OD from measurements and analysis of short-wave broadband irradiance. The predicted OD values are similar to those obtained using the algorithm of Min and Harrison (1996). The medians of the OD distributions derived from the two methods for a given site differ by less than 10%. The main motivation for using this OD retrieval technique is that no ancillary measurements are required for its application. It also offers computational simplicity. Still the Barnard et al. (2003) algorithm has some notable limitations. Similar to the Min and Harrison (1996) technique, the Barnard et al. (2003) method is designed for application only for single-layer overcast skies over surfaces with albedos less than 0.3 when the cosine of the solar zenith angle is greater than 0.15.

Cloud top and base heights were derived from the ARM SCF ceilometer, radar, and lidar data using the active remote sensing cloud layer (ARSCL) algorithm (Clotheaux et al. 2000). Cloud LWP was derived using the method of Liljegren et al. (????) for overcast clouds only (?).

To ensure time scale consistency between the data sets and to match the times when satellite data are available, all ground based retrievals at the SCF were averaged over the 15-minute intervals centered on the times when GOES data are available (every 15 minutes before and after each hour). All relevant data taken during the year 2000 are used in this study.

Satellite Retrievals

The satellite data consist of cloud properties retrieved from GOES-8 4-km radiances using VISST (Minnis at al. 1995a, 2001). It uses the GOES-8 imager 0.65-μm visible (VIS), 3.9-μm solar infrared (SIR), 10.8-μm, infrared (IR); and 12.0-μm split-window (SWC) channels taken every 15 to 30 minutes. VISST is used for near-real-time derivation of cloud and radiation properties during the daytime over the ARM SGP domain (32°N - 42°N; 91°W - 105°W). Each pixel is classified as clear or cloudy using a modified version of the cloud identification algorithm (Trepte et al. 1999). For each cloudy pixel,

VISST retrieves the cloud phase, OD, effective particle size, ice or LWP, the top, effective, and base height, and the cloud top temperature. The microphysical properties are estimated using the modeled cloud parameterizations of Minnis et al. (1998). Cloud thickness, used to determine cloud base height, is estimated using the formulation of Chakrapani et al. (2001). For clear pixels, the algorithm derives the clear-sky temperatures and visible-channel albedos. The broadband SW albedo and outgoing LW radiation (OLR) are estimated for all pixels.

Determination of the cloud properties requires an array of various input data. Clear-sky VIS reflectance at a given time and location is computed by applying solar zenith angle (SZA) dependent albedo models and bidirectional reflectance models to a database of clear-sky zenith-sun albedos resolved at 10' of latitude and longitude (Trepte et al. 1999). A similar database for the surface emissivity at SIR, IR, and SWC wavelengths is also maintained to help predict the clear-sky temperatures for these channels at any given time and location (Smith et al. 1999). Water-land percentage and elevation maps are used to determine the surface type and atmospheric thickness, respectively, for each grid location. Temperature and humidity profiles are interpolated from the gridded rapid update cycle (RUC; see Benjamin et al. 2004) analyses to match the analysis grid and image times. Surface skin temperature is estimated from the RUC surface air temperature with an update of the technique used by Minnis et al. (1995b). The RUC vertical profiles of temperature and humidity are used to account for attenuation of the reflected and emitted radiances as they pass through the atmosphere in direction of the satellite. The temperature profiles are also used to assign a cloud top height to the derived cloud temperature. All of the VISST cloud parameters are computed only during daytime (SZA <78°).

Spatial Averaging and Pixel Collocation

Combining data from more than one instrument requires some method for taking into account the differences in the field of view (FOV). Each IR GOES pixel is an ellipse with a nominal diameter of 4 km; hence the cloud properties are retrieved at a nominal spatial resolution of 4 km. The size of the "footprint" of the FOV of the ground-based SIRS instruments in the plane of the cloud will vary and depends on the FOV itself and on the cloud height. An accurate point-to-point comparison of satellite and ground-based cloud properties requires appropriate spatial averaging and interpretation of the available data sets. Figure 1a illustrates the approach taken in this study.

For simplicity, the overcast case is considered first. Long and Ackerman (1999) estimate an effective FOV $\alpha = 160°$ for SIRS based on experiments of sensitivity and contribution of energy to the flat plate detector at glancing incidence. If a cloud field is located at cloud height Hc, the SIRS will "see" a circle with radius:

$$R = Hc * \tan(\alpha / 2), \quad (1)$$

where Hc is the cloud field height retrieved from GOES. All pixels within a distance less or equal to R will fit in the circle seen by SIRS. The cloud properties derived by VISST for these GOES pixels will be appropriately averaged deriving a set of cloud properties to compare to the ground based retrievals. These pixels altogether are equivalent to a smaller and more precisely localized area than any other known studies to date.

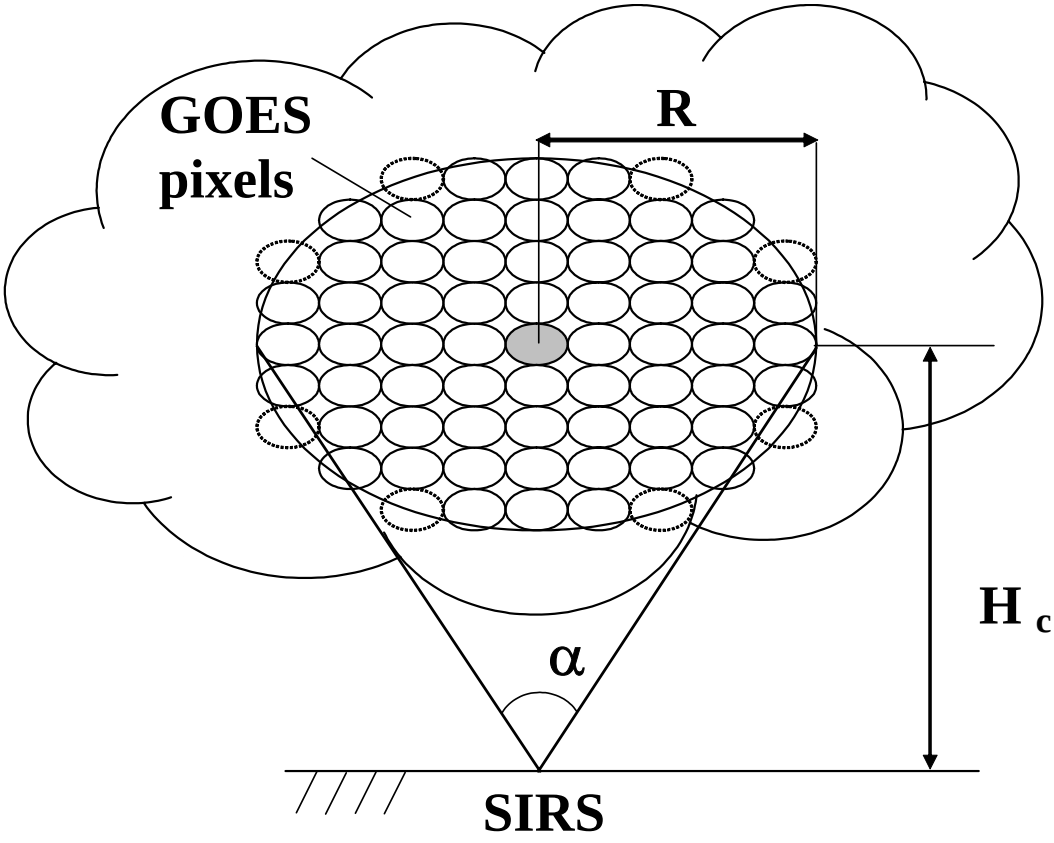

Figure 1a. The point-to-point comparison approach illustration.

The above procedure suggests how many pixels should be used for comparison to the surface data. The next step is to determine which pixels should be included. Due to factors such as uncertainties in satellite navigation, the assigned latitude and longitude may be erroneously given to an adjacent pixel located, say, within 3 pixels north, south, east or west of the actual location. Another consideration is the GOES viewing zenith angle (VZA) and the attendant parallax effect. While SIRS looks straight up centered on nadir, GOES views the SCF from VZA = 48° in the northwest direction. Because of this VZA, the GOES actually views the clouds located slightly southeast of the SCF when the SCF coordinates are specified. The amount of parallax shift depends on the cloud height. This dislocation is more significant for higher cloud fields and when winds in NW-SE directions are present, as illustrated in Figure 1b.

In addition to the collocation problems described above, it is necessary to reconcile the various instruments' FOVs. SIRS provides hemispherical sky cover and an angular-based view of the amount of the sky containing clouds (??), while GOES cloudy and clear pixels are used to calculate a cloud amount based on the number of pixels that contain clouds. GOES cloud amounts are not necessarily the true "cloud fraction," which is assumed to be the fraction of the area that is covered by cloud as projected

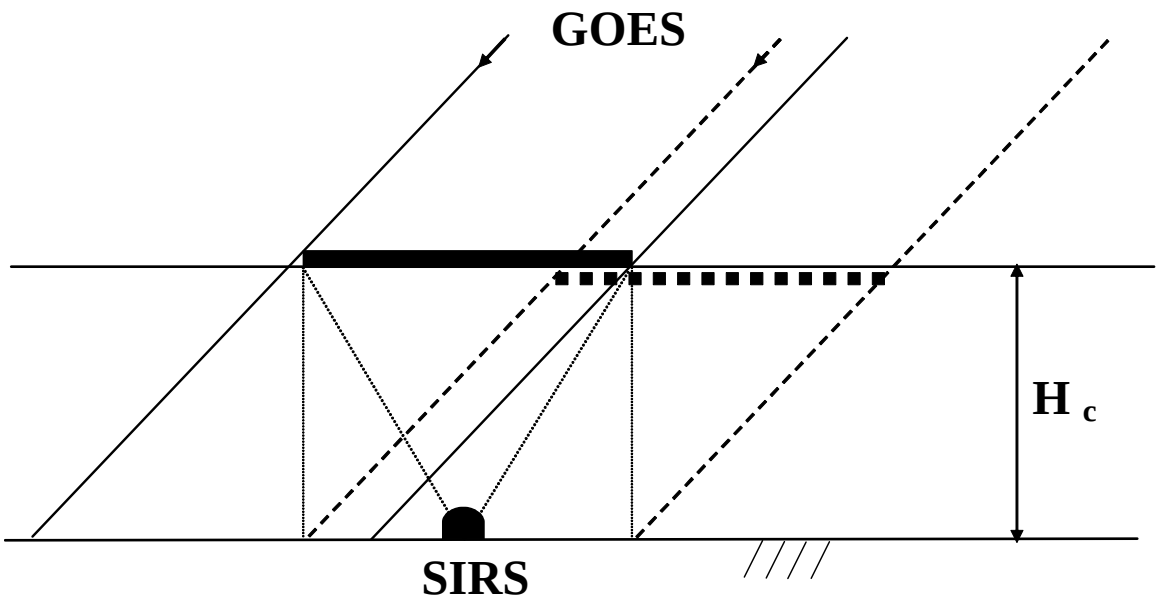

Figure 1b. Parallax effect caused by the satellite VZA.

straight down onto the surface. This concept is shown in Figure 1c. The VZA dependence of cloud amount from GOES is an important consideration in cloud cover quantification (Minnis 1989). Kassianov and Long (2003) differentiate between hemispherical sky cover and nadir-view cloud fraction for two reasons. The first reason is the difference in observational views: orthogonal (XYZ) viewpoint for nadir cloud fraction versus the angular viewpoint for the hemispherical sky cover. The second reason is the sensitivity to the 3D structure of the cloud, i.e., cloud fraction is independent of vertical/horizontal cloud variability while the hemispherical sky cover is. In order to overcome the differences between cloud fraction (nadir viewed), sky cover (hemispherical), and satellite cloud amount one can include ancillary data for the cloud aspect ratio and apply temporal averaging. However, both the satellite cloud amount for the SGP sites from the slanted view at those latitudes, and the hemispheric sky cover from the surface, tend to be overestimates compared to the "true" cloud fraction, CF. The reason, as explained in Kassianov and Long (2004), is related to the probability of a clear line of sight being a monotonically decreasing function of zenith viewing angle. The rate of decrease of this probability depends on the vertical/horizontal cloud distribution. But in the case of collocated satellite and surface cloud amount estimates of the same cloud field, both are similarly biased higher than actual nadir cloud fraction.

Given the above complications it is impossible to deconvolve the effects of each effect individually at the Extended Facilities due to the lack of the necessary ancillary information. Thus, a generalized approach is used to refine the pixel location assignment. The given latitude and longitude from VISST are first assumed to be nominally correct. After obtaining a cloud height for the specified location, the VISST cloud properties are averaged over the number of pixels within a radius R that defines the circle corresponding to the SIRS effective FOV. This initial location is used as a starting point to find an optimal collocation between the satellite pixels and the surface FOV by minimizing the difference in cloud amount between the two measurements, a procedure designated collocation by cloud amount. The

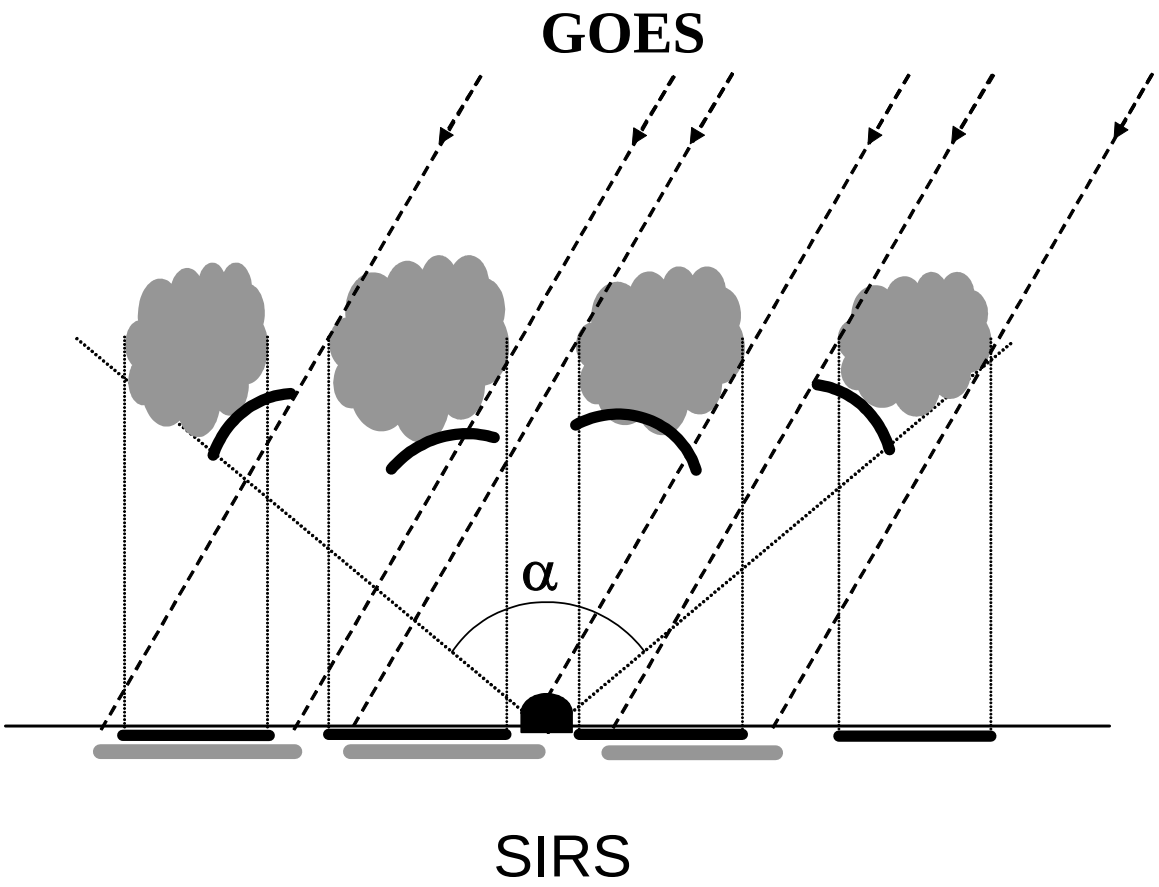

Figure 1c. Differences between nadir view cloud fraction (shown with gray bars), hemispherical sky cloud cover (shown with black arches) and VZA influenced satellite cloud amounts (shown with black bars).

difference between the satellite cloud amount and surface-retrieved sky cover is computed using the initial location. The satellite cloud amount is then recomputed for different locations around the initial coordinates by shifting the center of the satellite pixels one pixel at a time in each direction by up to 4 pixels. The shift that minimizes the difference between the surface and satellite cloud amounts defines the satellite area of collocation. The resultant collocated area is used to extract the full set of cloud properties from GOES for comparison to the surface data. For overcast cases (CF >0.9), the optimal collocation minimizes the OD differences in a manner similar to that described above for cloud amount. Fortunately, the surface-based Barnard et al. (2003) method retrieves cloud ODs under overcast conditions.

The main uncertainty of the described spatial averaging and pixel collocation technique is the accuracy of the cloud height Hc used to calculate R. For instance, an error of 2 km in the cloud height will change R by up to 6 km; hence the number of GOES pixels to be used will be different. We explored the possibility of using different cloud heights, i.e. cloud base, effective radiative height, or center height Hcen defined as follows:

$$Hcen = Hb + (Ht - Hb) / 2. \quad (2)$$

An analysis using Hb, Ht, and Hcen indicated that Hcen provides the highest degree of correlation between the satellite and ground based cloud amounts and OD comparison. Thus, the center height Hm is used to produce the results presented below.

Results and Discussion

Collocation by Cloud Amount and Optical Depth

The spatial averaging and pixel collocation approach was applied to data from the ARM SCF and GOES-8 for the year 2000. The results are shown in Figures 2 - 5. The dataset excludes cases when one or more of the needed quantities (cloud mask and OD from GOES; SWFA sky cover, surface retrieved OD) were not available.

The scatter plot in Figure 2a compares the individual satellite and surface retrieved cloud amounts. The solid line represents the line of agreement while the dashed lines represent +/- one standard deviation from the line of agreement (this notation will hold true for the rest of this study)**.** The cloud amount difference kurtosis is very high (k = 11.14); thus more than 75% of the cases fall into the range of the red dashed lines. The histograms of CF from GOES and the surface prior to collocation (Figure 2b) are very similar for CF >0.6. About 75% of the cases show differences smaller than 10% cloudiness (Figure 2c) and about 55% of the cases, mostly overcast, exhibit even smaller differences of 5%. Of the remaining "badly matched" cloud amounts, 70% occur when SC <0.2. More than half of these differences are negative. They are caused by thin cirrus clouds or by partially cloud-filled pixels that do not alter the clear-sky radiance field sufficiently for detection by the cloud mask. Some of these differences are also due to false cloud detection by the SWFA in heavy aerosol conditions. Positive sign errors are associated with the presence of broken bright clouds or single fast moving cloud patches. Note, that the satellite retrievals are binary in nature; each 4 km pixel is designated as either completely filled or devoid of cloudiness.

Figure 3 is similar to Figure 2, but represents the comparison after applying collocation by cloud amount to the initial GOES data set. The scatter plot in Figure 3a reveals that more points are concentrated near the line of agreement and the kurtosis is twice the value found without collocation. This means 14% more points are within 1 standard deviation. However, neither the standard deviation relative to perfect agreement nor the correlation coefficient are negligibly different from their counterparts for the raw dataset. This means that the collocation cannot correct for the inherent cloud masking algorithm limitations. The similarity between the cloud amount histograms (Figure 3b) is improved by collocation for the lower cloud amounts, 0.1<CF<0.4. Collocation increases the number of cloud amount differences less than 5% from 55% to 70% (Figure 3c). The method also improves the agreement for overcast cases, which confirms that the satellite spatial resolution (pixel size) limitation is a major cause for erroneous satellite cloud amounts.

The scatter plot in Figure 4a compares the satellite and surface retrieved OD datasets. About 80% of the cases fall into the range of the dashed lines. The data are not pre-screened by the number of cloud layers present, since this may reduce significantly the number of cases available and the statistics

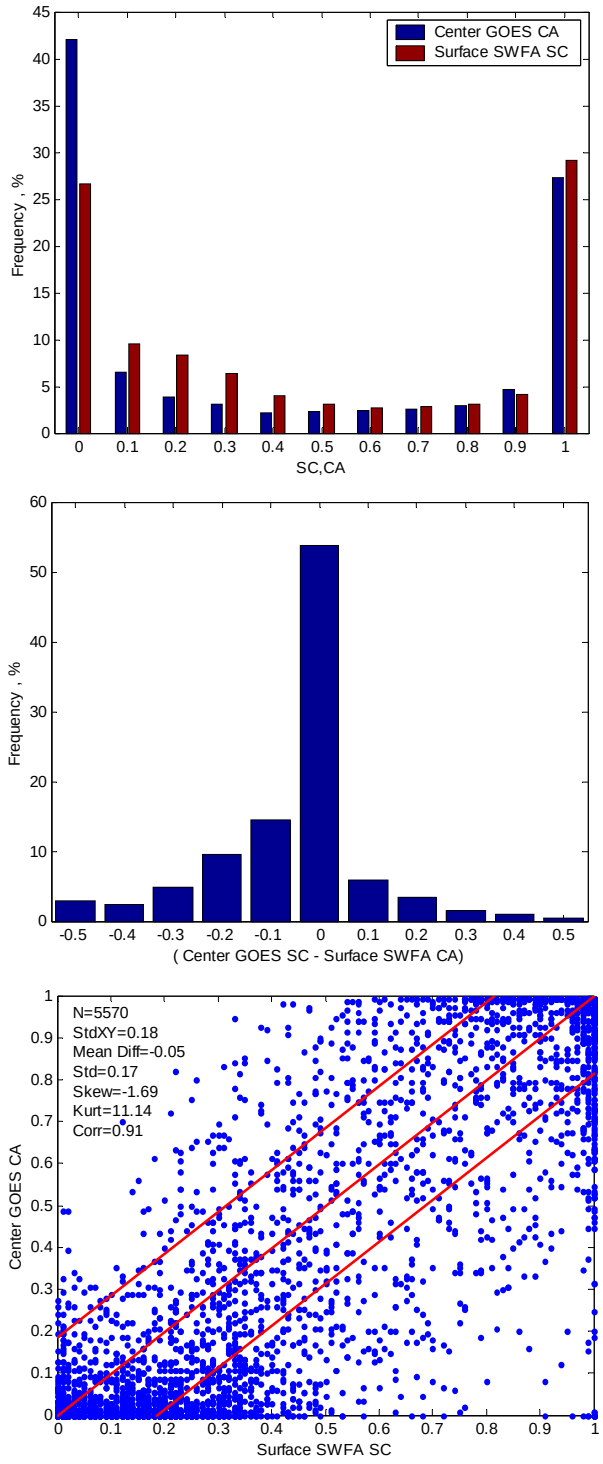

Figure 2. (a) Distribution of satellite cloud amounts and SWFA sky covers for year 2000, (b) differences distribution for the same year, and (c) scatterogram of satellite cloud amounts vs. SWFA sky cover for the same year.

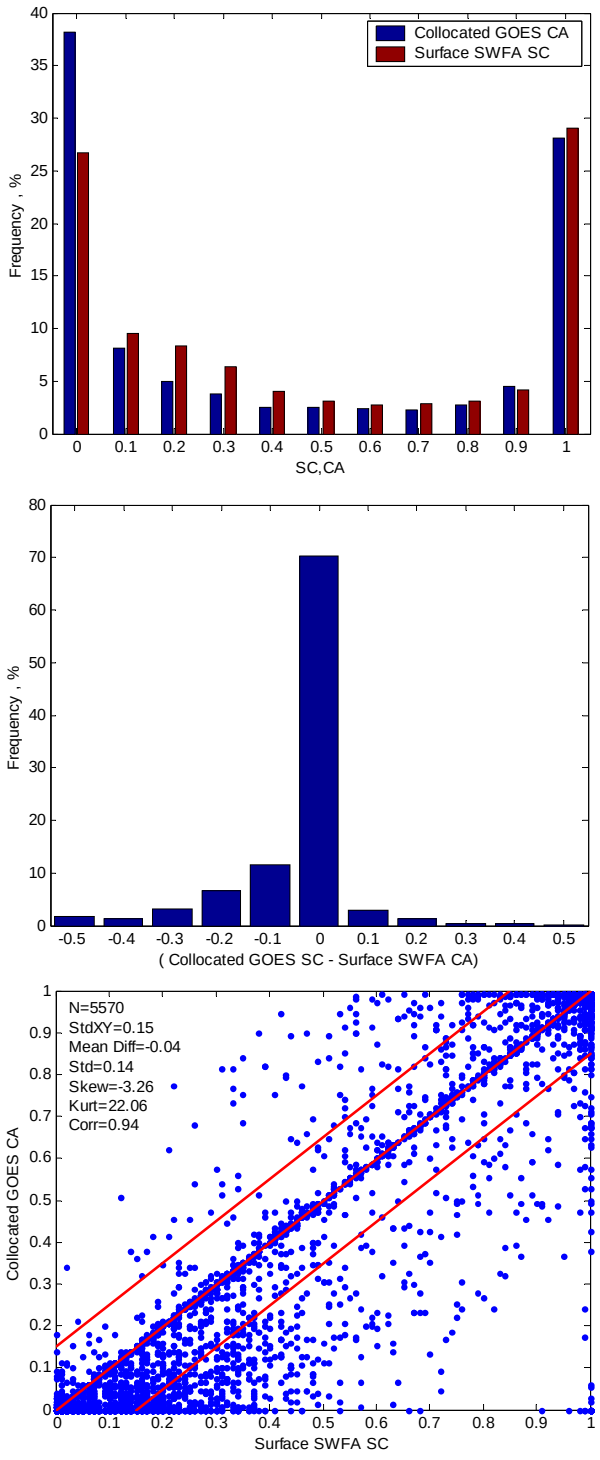

Figure 3. (a) Distribution of collocated satellite cloud amounts and SWFA sky covers for year 2000, (b) differences distribution for the same year, and (c) scatterogram of collocated satellite cloud amounts vs. SWFA sky cover for the same year.

will not be representative. The distributions of ODs and the differences between satellite and surface for the year 2000 are illustrated in Figures 4b and 4c, respectively, prior to collocation. As mentioned earlier, due to the limitation of the ground-based cloud OD retrieval technique only overcast cases (CA>0.9) are included.

A significant number of the cases showing OD difference of 10 and more are multi-layer cases. Cloud layer height analysis as estimated from the ARSCL dataset shows that when the two layers are vertically quite distant from each other, i.e., the separation is larger than the geometrical thickness of either layer; the OD error is often greater than 100%. This study reduces the impact of one practical limitation of the Min and Harrison (1996) algorithm, which by methodology is of limited certainty for retrieving ODs below a value of about 10. The Barnard and Long (2004) method, using broadband SW data, is theoretically less affected by this limitation and should be applicable for optical thickness between 3 and 150.

The scatter plot of the collocated data in Figure 5c shows improved statistics, with kurtosis rising from 6.9 (Figure 4c) to 10.8. The standard deviation decreased from 20 to 15 and the correlation coefficient increased from 0.70 to 0.82. Histograms of OD and differences after collocation are plotted in Figures 5b and 5c, respectively. Similarly to the cloud amounts, there is improvement in the comparison of OD histograms, especially for OD smaller than 30. There is a significant increase in the number of cases with optical thickness differences of 10 or less, increasing from 35% before to almost 60% of the cases after the collocation.

LWP, Hb, and Ht Intercomparison

The effects of the pixel collocation on the LWP and cloud heights are examined using the. Data from the year 2000 obtained at the ARM SGP central facility is used. The ground-based data is derived with the techniques explained in the previous section. The minimum cloud amount limit is 0.05. This is to avoid possible miscalculation deriving the empirical OD (Barnard at al. 2003). The cloud heights from GOES are compared to the cloud base and top heights from the ARSCL data. Either the cloud amount or OD collocation method was applied depending on the value of the surface cloud sky cover for each particular instance. Collocated LWP, Hb, and Ht were derived from the GOES data using the resultant minimizing shift.

The four panels in Figure 6 represent the results from intercomparing cloud amounts and cloud OD before and after the collocation. The cloud amount correlation increases from 0.50 to 0.92, while the corresponding OD correlation rises from 0.62 to 0.72. Figure 7 illustrates the LWP, cloud base and cloud top height comparisons. For these cloud properties single pixel satellite retrievals are compared to 15-minute averaged surface pencil-beam derived cloud properties. Due to the specifics of the VISST algorithm it is possible that LWP, Hb, and Ht may not be retrieved for every pixel, hence different number of cases is compared before and after the collocation. The statistics provided with every scatter plot reveal that the cloud LWP, cloud base, and top heights are not significantly improved after the collocation. This is illustrative of the fact that the temporal averaging of the surface retrievals cannot compensate for the spatial resolution difference of the various datasets and that the spatial mismatching remains to be a problem in point-to-point comparison of satellite and ground-based cloud properties. A careful visual examination of Figure 7 scatterograms shows higher concentration of

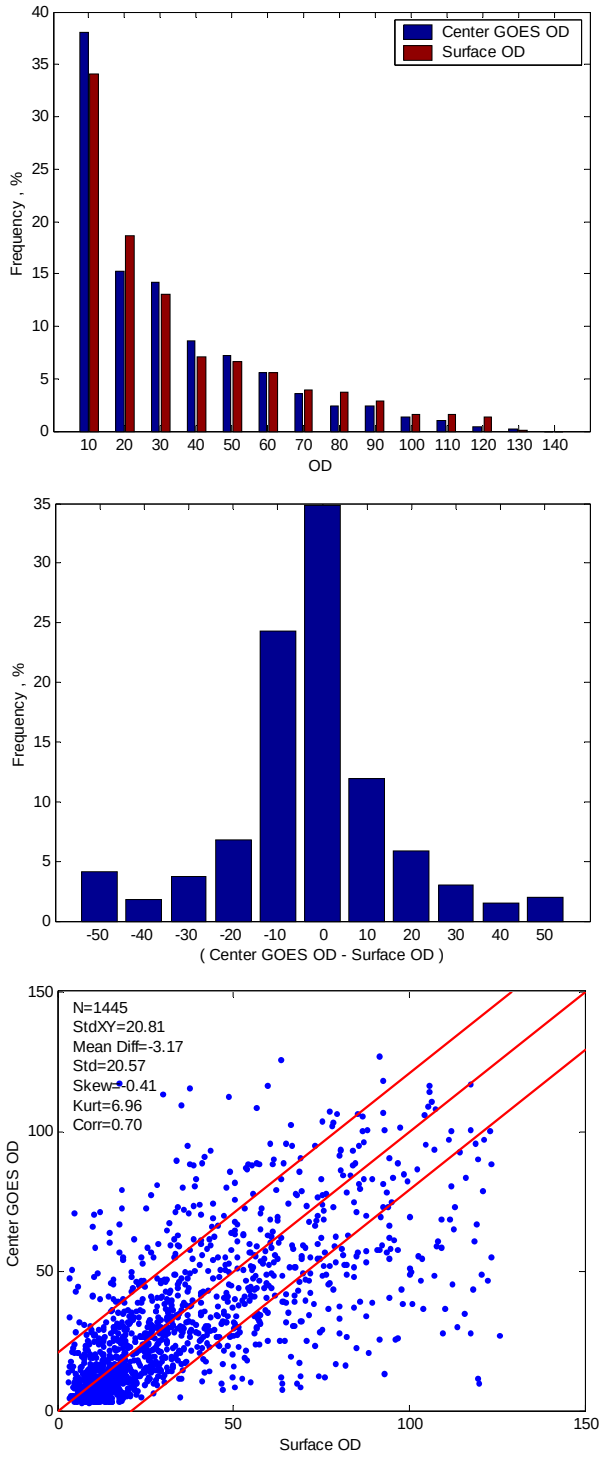

Figure 4. (a) Distribution of satellite and surface retrieved cloud ODs for year 2000, (b) differences distribution for the same year, and (c) scatterogram of satellite vs. surface retrieved cloud OD for the same year.

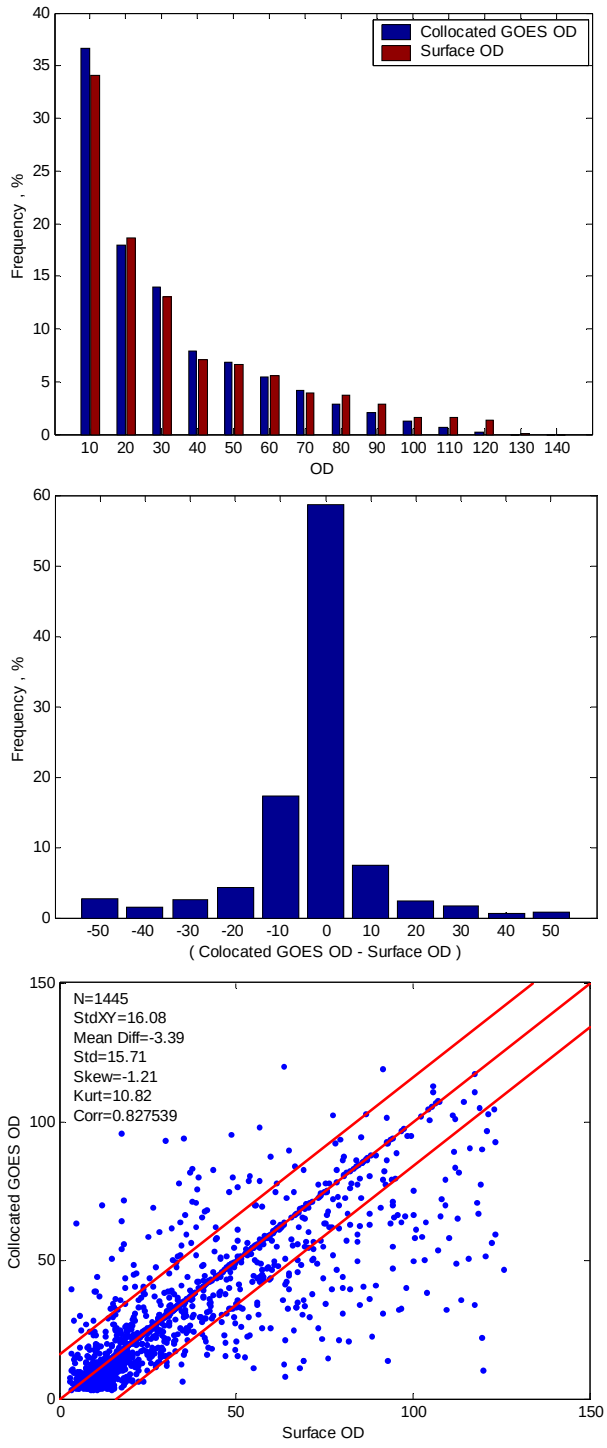

Figure 5. (a) Distribution of collocated satellite and surface retrieved cloud ODs for year 2000, (b) differences distribution for the same year, and (c) Scatterogram of satellite vs. surface retrieved cloud ODs for the same year.

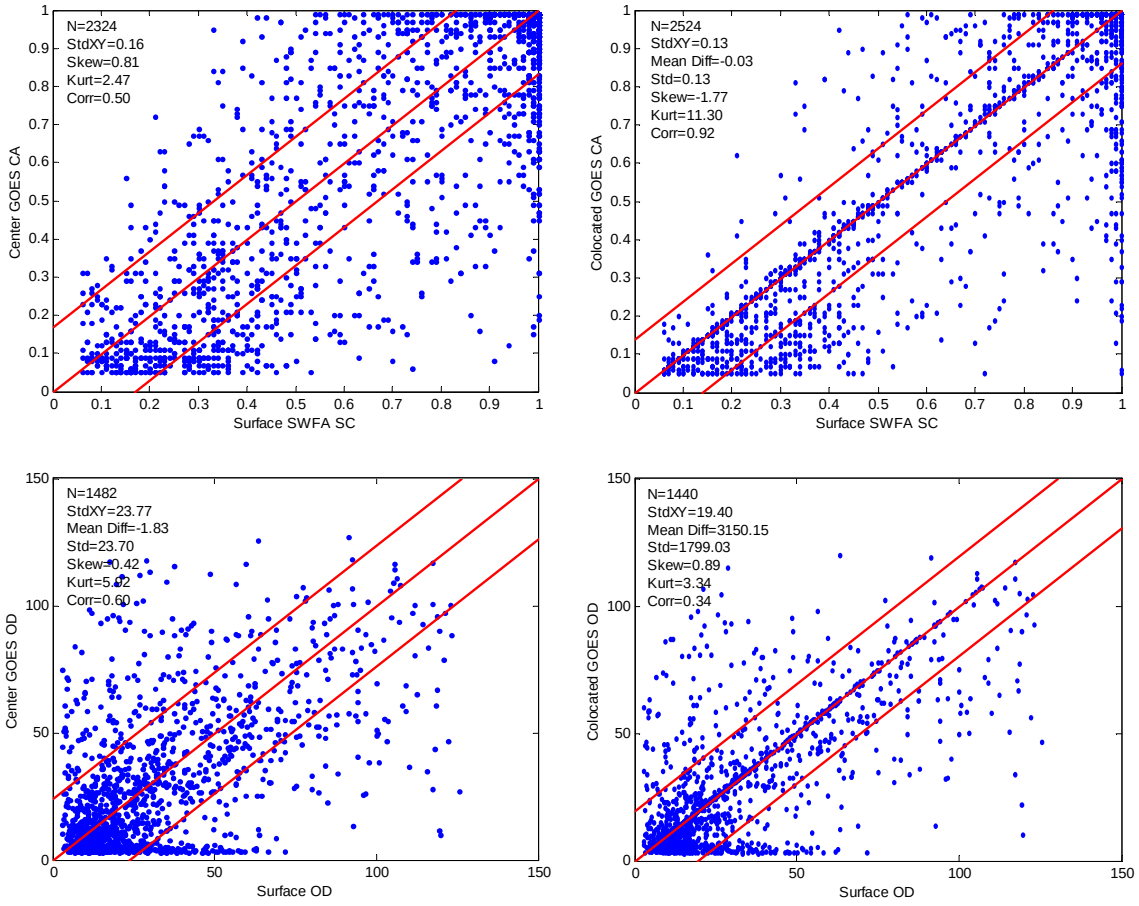

Figure 6. Cloud amount and ODs comparison for SGP CF, year 2000, before (on the left hand side) and after (on the right hand side) applying a collocation.

points close to the X = Y fit. The ranges of improved alignments are from 0 to 200 g/m^2 for LWP, from 2000 to 8000 meters for Hb, and from 1000 to 10 000 meters for Ht. This proves that the collocation approach effective, despite the fact that each retrieval uncertainty may be predominant contributor to the differences between the surface and the satellite retrievals.

Conclusions

This work presents a methodology for point-to-point comparison of satellite and ground-based cloud properties. The methodology was employed for one year of data analysis for the ARM SGP central facility. We compared cloud amounts and ODs retrieved with GOES VISST and surface methods, and evaluated the differences. After applying spatial averaging and pixel collocation to the initial GOES data we estimated mean difference and difference standard deviation, respectively, of -0.04 and 0.15 for the cloud amounts, and -3.39 and 16.08 for the OD. Outlining the conditions under which GOES cloud amounts and ODs are consistent with the surface retrievals improves the interpretation of GOES-VISST derived cloud properties. LWP and cloud heights intercomparison shows limited improvement of the agreement between the satellite and ground based

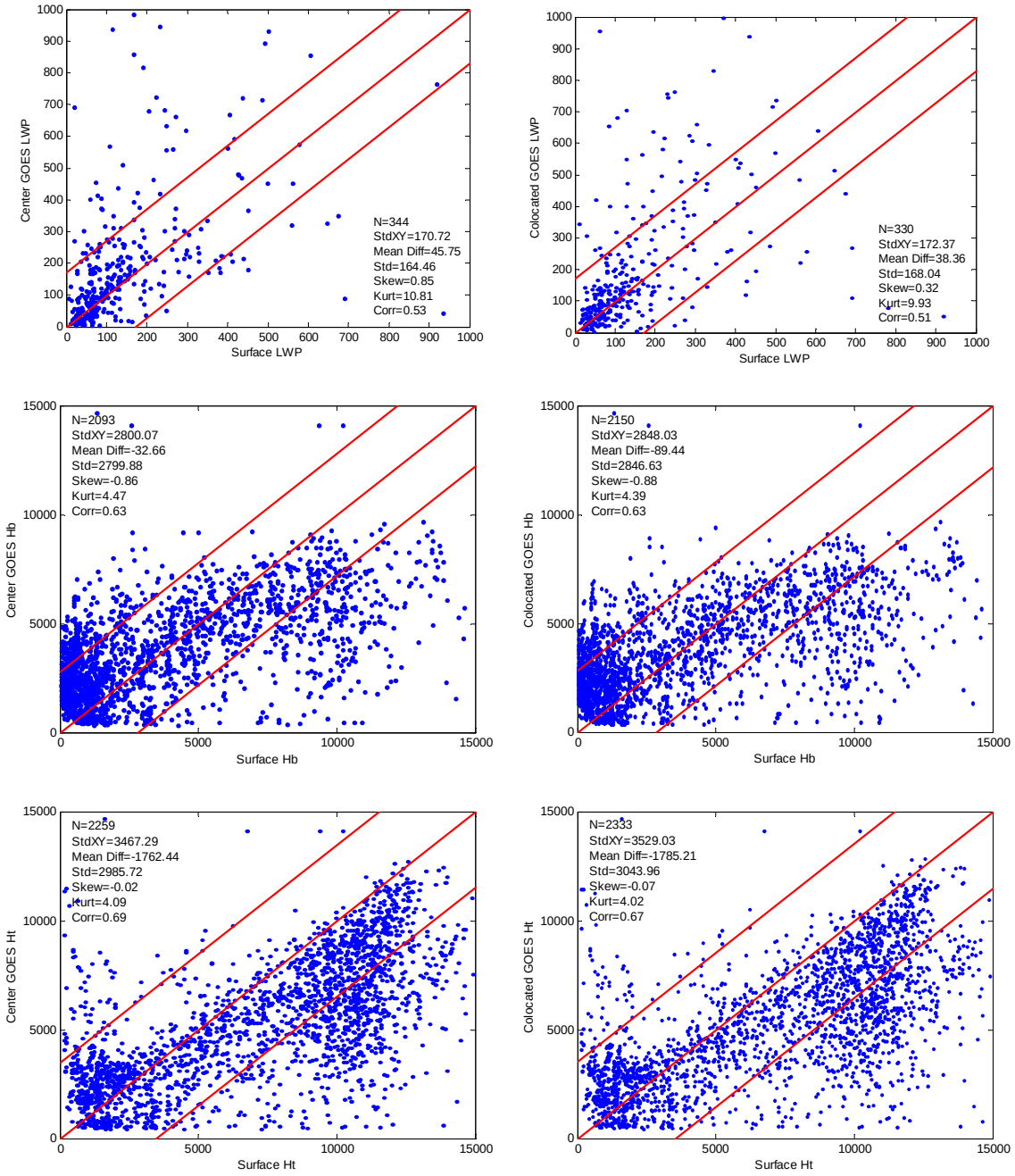

Figure 7. LWP, cloud base and top height comparison for SGP CF, year 2000, before (on the left hand side) and after (on the right hand side) applying a collocation.

retrievals, however the collocation approach was proven to successful for certain ranges of LWP, Hb, and Ht. The methodology for point-to-point comparison of satellite and ground-based cloud properties will now be used in our research for the comparison of satellite and surface data for the ARM SGP Extended Facilities with the aim of producing column profiles of cloud properties.

Acknowledgements

This research was supported by the U.S. Department of Energy Atmospheric Radiation Measurement Program under Interagency Agreement DE-AI01-02ER6331.

Corresponding Author

Iliana Genkova, iliana.genkova@pnl.gov, (509) 372-6020

References

Ackerman and Stokes, 2003: ??

Barnard, J., and C. Long, 2004: A simple empirical equation to calculate cloud optical thickness using shortwave broadband measurements. *J. Appl. Meteorol.*, accepted.

Benjamin, S. G., and authors, 2004: An hourly assimilation – forecast cycle: The RUC. *Mon. Wea. Rev.*, **132**, 495–518.

Chakrapani, V., D. R. Doelling, A. D. Rapp, and P. Minnis, 2002: Cloud thickness estimation from GOES-8 satellite data over the ARM SGP site. In *Proceedings of the Twelfth Atmospheric Radiation Measurement (ARM) Science Team Meeting*, ARM-CONF-2002. U.S. Department of Energy, Washington, D.C. Available URL: http://www.arm.gov/publications/proceedings/conf12/extended_abs/chakrapani-v.pdf

Clothiaux, E. E., T. P. Ackerman, G. G. Mace, K. P. Moran, R. T. Marchand, M. A. Miller, and B. E. Martner, 2000: Objective determination of cloud heights and radar reflectivities using a combination of active remote sensors at the ARM CART sites. *J. Appl. Meteorol.*, **39**, 645–665.

Dong, X., P. Minnis, G. G. Mace, W. L. Smith, Jr., M. Poellot, R. T. Marchand, and A. D. Rapp, 2002: Comparison of stratus cloud properties deduced from surface, GOES, and aircraft data during the March 2000 ARM Cloud IOP. *J. Atmos. Sci.*, **59**, 3256–3284.

Ho, S.-P., B. Lin, P. Minnis, and T.-F. Fan, 2003: Estimation of cloud vertical structure and water amount over tropical oceans using VIRS and TMI data. *J. Geophys. Res.*, **108**, 4419, 10.1029/2002JD003298.

Huang, J. P., M. M. Khaiyer, P. W. Heck, P. Minnis, and B. Lin, 2003: Determination of ice-water path over the ARM SGP using combined surface and satellite datasets. In *Proceedings of the Thirteenth Atmospheric Radiation Measurement (ARM) Science Team Meeting*, ARM-CONF-2003. U.S. Department of Energy, Washington, D.C. Available URL: http://www.arm.gov/publications/proceedings/conf13/extended_abs/huang-j.pdf

Kassianov E., C. Long, and M. Ovtchinnikov, 2003: Cloud sky cover versus cloud fraction: whole-sky simulations and observations. *J. Appl. Meteorol*., submitted.

Khaiyer, M. M., P. Minnis, B. Lin, W. L. Smith, Jr., and A. D. Rapp, 2003: Validation of satellite-derived liquid water paths using ARM SGP microwave radiometers. In *Proceedings of the Thirteenth Atmospheric Radiation Measurement (ARM) Science Team Meeting*, ARM-CONF-2003. U.S. Department of Energy, Washington, D.C. Available URL: http://www.arm.gov/publications/proceedings/conf13/extended_abs/khaiyer-mm.pdf

Ou, S. C., K. N. Liou, Y. Takano, G. G. Mace, K. Sassen, and A. Heymsfield, 2003: 3D remote sensing of cirrus cloud parameters using AVHRR and MODIS data coupled with radar and lidar measurements. In *Proceedings of the Thirteenth Atmospheric Radiation Measurement (ARM) Science Team Meeting*, ARM-CONF-2003. U.S. Department of Energy, Washington, D.C.

Long, C. N., and T. P. Ackerman, xxxx: Identification of clear skies from broadband pyranometer measurements and calculation of downwelling shortwave cloud effects. *J. Geophys. Res.*, **105**, 15,609-15,626.

Long, C., T. Ackerman, J. J. DeLuisi, and J. Augustine, 1999: Estimation of fractional sky cover from broadband SW radiometer measurements. *Proc. AMS 10th Conf. on Atmos. Rad.*, Madison, Wisconsin, June 28 – July 2, 1999.

Long, C., D. Slater, and T. Tooman, November 2001: *Total Sky Imager (TSI) Model 880 Status and Testing Results*, ARM-TR-006. Available URL: http://www.arm.gov/publications/tech_reports/arm-tr-006.pdf

Min, Q., and L. C. Harrison, 1996: Cloud properties derived from surface MFRSR measurements and comparison with GOES results at the ARM SGP Site. *Geophys. Res. Lett.*, **23**, 1641–1644.

Min, Q., and P. Minnis, 2004: Comparison of cirrus optical depths from GOES-8 and surface measurements. *J. Geophys. Res.*, accepted.

Minnis, P., and authors, 1995a: Cloud Optical Property Retrieval (Subsystem 4.3). "Clouds and the Earth's Radiant Energy System (CERES) Algorithm Theoretical Basis Document, Volume III: Cloud Analyses and Radiance Inversions (Subsystem 4)," *NASA RP 1376 Vol. 3*, edited by CERES Science Team, pp. 135–176.

Minnis, P. and W. L. Smith, Jr., Cloud and radiative fields derived from GOES-8 during SUCCESS and the ARM-UAV Spring 1996 Flight Series. *Geophys. Res. Lett.*, **25**, 1113-1116, 1998.

Minnis P., W. L. Smith, Jr., D. P. Garber, J. K. Ayers, and D. R. Doelling, 1995b: *Cloud properties Derived from GOES-7 for Spring 1984 ARM Intensive Observing Period using Version 1.0.0 of ARM Satellite Data Analysis Program*, NASA RP 1366, p. 58.

Minnis, P., W. L. Smith, Jr., D. F. Young, L. Nguyen, A. D. Rapp, P. W. Heck, S. Sun-Mack, Q. Trepte, and Y. Chen, 2001: A near-real time method for deriving cloud and radiation properties from satellites for weather and climate studies. *Proc. AMS 11th Conf. Satellite Meteorology and Oceanography*, Madison, Wisconsin, October 15-18, 2001, pp. 477-480.

Piironen, A., and E. W. Eloranta, 1995: Convective boundary layer mean depths, cloud base altitudes, cloud top altitudes, cloud coverages, and cloud shadows obtained from volume imaging lidar data. *J. Geophys. Res.*, **100**, 25,569–25,576.

Smith, W. L., Jr., P. Minnis, D. F. Young, and Y. Chen, 1999: Satellite-derived surface emissivity for ARM and CERES. *Proc. AMS 10th Conf. Atmos. Rad.*, Madison, Wisconsin, June 28 – July 2, 1999, pp. 410-413.

Stokes, G. M., and S. E. Schwartz, 1994: The Atmospheric Radiation Measurement (ARM) Program: Programmatic background and design of the cloud and radiation test bed. *Bull. Am. Meteor. Soc.*, **75**, 1201–1222.

Trepte, Q., Y. Chen, S. Sun-Mack, P. Minnis, D. F. Young, B. A. Baum, and P. W. Heck, 1999: Scene identification for the CERES cloud analysis subsystem. *Proc. AMS 10th Conf. Atmos. Rad.*, Madison, Wisconsin, June 28 – July 2, 1999, pp. 169–172.